Src-family kinases stabilize the neuromuscular synapse in vivo via protein interactions, phosphorylation, and cytoskeletal linkage of acetylcholine receptors

Abbreviated title: Src action in postsynaptic stabilization

Gayathri Sadasivam*, Raffaella Willmann*, Shuo Lin§, Susanne Erb-Vögtli*, Xian Chu Kong§, Markus A. Rüegg§, and Christian Fuhrer*

*Department of Neurochemistry, Brain Research Institute, University of Zürich, Winterthurerstrasse 190, CH-8057 Zürich, Switzerland

§Biozentrum, University of Basel, Klingelbergstrasse 70, CH-4056 Basel, Switzerland

Address for correspondence: Christian Fuhrer, Brain Research Institute, University of Zürich, Winterthurerstrasse 190, CH-8057 Zürich, Switzerland. Tel.: +41 44 635 33 10. Fax: +41 44 635 33 03. E-mail: chfuhrer@hifo.unizh.ch

Number of Figures: 10; 1 Supplementary Figure; Number of pages: 32
Key words: Src, acetylcholine receptor, neuromuscular synapse, agrin, tyrosine-phosphorylation, postsynaptic membrane

Abstract

Postnatal stabilization and maturation of the postsynaptic membrane are important for development and function of the neuromuscular junction (NMJ), but the underlying mechanisms remain poorly characterized. We have examined the role of Src-family kinases (SFKs) in vivo. Electroporation of kinase-inactive Src constructs into soleus muscles of adult mice caused NMJ disassembly: acetylcholine receptor (AChR)-rich areas became fragmented, the topology of nerve terminal, AChRs and synaptic nuclei was disturbed, and occasionally nerves started to sprout. Electroporation of kinase-overactive Src produced similar but milder effects. We studied the mechanism of SFK action using cultured $src^{-/-};fyn^{-/-}$ myotubes, focusing on clustering of postsynaptic proteins, their interaction with AChRs, and on AChR phosphorylation. Rapsyn and the utrophin-glycoprotein complex were recruited normally into AChR-containing clusters by agrin in $src^{-/-};fyn^{-/-}$ myotubes. But after agrin withdrawal, clusters of these proteins disappeared rapidly in parallel with AChRs, revealing that SFKs are of general importance in postsynaptic stability. At the same time, AChR interaction with rapsyn and dystrobrevin, and AChR phosphorylation decreased after agrin withdrawal from mutant myotubes. Unexpectedly, levels of rapsyn protein were increased in $src^{-/-};fyn^{-/-}$ myotubes, while rapsyn-cytoskeleton interactions were unaffected. The overall cytoskeletal link of AChRs was weak but still strengthened by agrin in mutant cells, consistent with the normal formation but decreased stability of AChR clusters. These data show that correctly balanced activity of SFKs is critical in maintaining adult NMJs in vivo. SFKs hold the postsynaptic apparatus together through stabilization of AChR-rapsyn interaction and AChR phosphorylation. In addition, SFKs control rapsyn levels and AChR-cytoskeletal linkage.

NMJs develop in a series of steps in which the postsynaptic membrane first forms by concentrating AChRs and associated proteins in a flat topology. Postnatally, NMJs mature and AChRs get arranged at the crests of postjunctional folds. Concomitantly, all but one axon withdraw, paralleled by destabilization of adjacent AChRs (Sanes and Lichtman, 2001). Maturation and stabilization of AChR clusters ensure proper synaptic development, which forms the basis for nerve-evoked muscle contractibility.

Much is known about the molecular pathways that first form NMJs. Neural agrin, by activating the kinase MuSK, is crucial by triggering downstream cascades (reviewed by (Bezakova and Ruegg, 2003; Luo et al., 2003). Central in these is rapsyn, the main AChR-anchoring protein mediating clustering (Gautam et al., 1995). Rapsyn increasingly binds to AChRs in response to agrin (Moransard et al., 2003), mediates agrin-induced phosphorylation of the AChR β and δ subunits (Mittaud et al., 2001), and links the receptor to β-dystroglycan, a component of the postsynaptic utrophin-glycoprotein complex (UGC) (Cartaud et al., 1998; Bartoli et al., 2001). In clustering, AChRs become immobilized and less detergent extractable, both in agrin-treated myotubes (Prives et al., 1982; Stya and Axelrod, 1983; Podleski and Salpeter, 1988) and developing NMJs (Dennis, 1981; Slater, 1982). The players in this cytoskeletal link remain uncertain. Agrin-induced phosphorylation of AChR β is involved (Borges and Ferns, 2001) and can occur through Abl and Src-family kinases (Finn et al., 2003; Mittaud et al., 2004).

Much less is known about the mechanisms that mature NMJs and stabilize AChR clusters postnatally. Although MuSK is required (Kong et al., 2004), some of these pathways may not be essential in initial NMJ formation (Willmann and Fuhrer, 2002), as illustrated by mice lacking utrophin and dystrophin or the UGC components α-dystrobrevin or dystroglycan (Grady et al., 1997; Grady et al., 2000; Jacobson et al., 2001). In these mice, NMJs form but fail to mature properly. In *α-dystrobrevin*^{-/-} mice, AChR clusters are normal at birth but increasingly fragment postnatally. Similarly, in cultured *α-dystrobrevin*^{-/-} myotubes, agrin induces normal AChR clustering, but these clusters are unstable and disperse rapidly when agrin is withdrawn from the myotubes (Grady et al., 2000). Thus, the UGC is a core player in postnatal NMJ stabilization. Further candidates are Src-family kinases (SFKs). In *src*^{-/-}*;fyn*^{-/-} mice, NMJs appear normal around birth, when the animals die. In cultured *src*^{-/-}*;fyn*^{-/-} myotubes, agrin and laminin induce normal AChR aggregation, but the clusters disperse rapidly upon withdrawal of these factors (Smith et al., 2001; Marangi et al., 2002).

To elucidate the mechanisms of synaptic stabilization, we have investigated the role of SFKs in vivo. In adult myofibers expressing dominant-negative Src, AChR-rich areas were severely

fragmented. We addressed the mode of SFK action in AChR cluster stabilization using $src^{-/-};fyn^{-/-}$ myotubes. We found that Src and Fyn maintain clusters of rapsyn and UGC components, maintain AChR-rapsyn interactions and AChR β phosphorylation, mediate AChR-cytoskeletal linkage and control rapsyn protein levels. Our data introduce SFKs as critical players in NMJ stabilization in vivo and reveal that complex signaling pathways underlie stabilization.

Materials and Methods

Src constructs, electroporation, whole mount preparation and immunohistochemistry.
Three different mutant Src expression constructs, each containing a CMV promoter, and an empty pLNCX control vector were used for electroporation into the soleus muscle of mice. Src-AM (Kaplan et al., 1994) was kindly provided by Dr. Pam Schwartzberg (NIH). Src-K295M (Mohamed et al., 2001) was received from Dr. Sheridan Swope (Georgetown University, Washington DC), and Src-Y527F from Dr. Joan Brugge (Harvard Medical School, Boston). Mutant Src constructs (8 µg/µl) and GFP containing a nuclear localization signal (NLS-GFP; 4 µg/µl) were mixed to yield final DNA concentrations of 2:1 (Src:GFP), and were first injected extrasynaptically into the soleus muscle of adult C57BL/6 mice (3-6 months). The wound was closed, electrodes were mounted against the leg, and electroporation was performed as described previously (Kong et al., 2004) using an ECM 830 electroporation system (BTX, Holliston, MA). Eight pulses of 20 ms were applied at a frequency of 1 Hz with voltage set to 200 V/cm. At the site of DNA injection, electroporation efficiency is highest, and once DNA constructs have entered muscle fibers, they diffuse within those to regions including the synapse (Kong et al., 2004). The electroporated muscles were analyzed after 6 weeks. Muscles were dissected and injected with 2% para-formaldehyde solution for fixation. This treatment is optimal for whole-mount analysis, as it swells the muscle, widening gaps between individual muscle fibers, facilitating further fiber dissection. Fixed tissue was teased into thin fiber bundles of 5-10 myofibers. Whole mount preparations were triple-labeled as described earlier (Kong et al., 2004). Briefly, AChRs were stained to visualize NMJs using rhodamine-coupled α-bungarotoxin. A mixture of rabbit polyclonal antibodies against neurofilament (Sigma, USA) and synaptophysin (Dakocytomation, Denmark), followed by Cy5-conjugated goat anti-rabbit or Alexa 350 goat anti-rabbit antibodies, was used to visualize motorneurons and nerve endings. The green channel was reserved for GFP. For cytoskeletal stainings, Alexa-350-coupled phalloidin (Molecular Probes, Eugene, USA) was used to label F-actin. Monoclonal anti-α-tubulin antibodies (clone DM1A from Sigma, Missouri, USA), followed by Cy5-conjugated goat anti-mouse antibodies, were used to visualize synaptic tubulin rings beneath the endplate. Conventional fluorescence imaging was done using a Zeiss Axioskop 2 microscope equipped with a Hamamatsu Orcacam digital camera.

Immunohistochemistry on cross-sections. Soleus muscle tissue prepared and fixed for whole-mount analysis (see above) was first placed overnight in 10% sucrose at 4°C and then embedded into O.C.T. (Tissue-Tek; Sakura Finetek, Zoeterwoude, NL). The tissue was frozen in a cooling

chamber (maintained at -4°C with surrounding liquid nitrogen) containing isopentane (Fluka, Germany) for approximately 5 minutes. Muscles were then cut into 14 μm cryosections (at -18°C). Sections were stained with rhodamine-coupled α-BT to visualize the AChRs at the NMJ. GFP signals were enhanced with polyclonal anti-GFP antibody (Molecular probes, Eugene, Oregon, USA) followed by Alexa 488-coupled goat anti-rabbit antibodies. Nuclei were visualized by DAPI (Hoechst nuclear stain; Molecular Probes).

The fixation procedure, optimized for whole mount analysis, expanded gaps between individual myofibers, rounding off some fibers and allowing entry of other cells (see Fig. 4C, D). Nonetheless, we could unequivocally identify muscle fibers (due to diffuse GFP-signal) and the positioning of nuclei within those fibers (as most of the strong nuclear GFP signals overlapped with DAPI).

Confocal microscopy, imaging and quantitation. Confocal laser scanning microscopy was performed using an inverted Leica confocal SP2 microscope coupled to a Silicon Graphics Workstation. A minimum of 40 stacks per image were taken, each section at approximately 0.3 μm thickness. These confocal stacks were shown as a maximal projection and eventually imported into a 3D image processing software, Imaris 4.1.1, for image reconstruction and rotation (Fig. 1-4). To quantify disassembly, synaptic contacts as visualized by the postsynaptic AChRs and the presynaptic nerve terminal were scored based on size and degree of disassembly. Intact endplates were large pretzel shaped structures (25 - 40 μm) and continuous along their contours. A partial disassembly was scored when the endplate was broken up into more than 2 main fragments and was porous. In such cases it was still possible to identify the parts of a pretzel. In a complete disassembly the structures completely dissolved into several fragments, which were less than 5 μm in length. These were scored as synaptic sites because of the nerve staining and surrounding intact endplates in GFP-negative fibers. Statistics were performed by averaging 3 sets of independent electroporation experiments, with a minimum of 30 pictures taken for each condition. In all cases the NLS-GFP signal colocalized with the AChR stain and lay beneath the endplates, suggesting that the electroporation was specific to the muscle nuclei and was not an indirect effect due to electroporation of Schwann cells. Apart from synaptic muscle nuclei, also extrasynaptic nuclei were GFP-positive in most cases.

Cell culture and agrin treatment. *src*^{-/-}*;fyn*^{-/-} cells (clones DM15 and DM11) and their corresponding wild-type cells (clones SW10 and SW5) were grown as described earlier (Smith et al., 2001), in DMEM supplemented with 2 mM glutamine, 10% fetal bovine serum, 10% horse

serum, 2% chick embryo extract, penicillin-streptomycin, and 20 U/ml recombinant mouse interferon-γ. In all assays we tested both mutant and both wild-type clones, also in pairwise comparison. There were no differences between clones of the same genotype, excluding the possibility of clonal variation.

For biochemical analysis, cells were plated on matrigel-coated tissue culture dishes (Nunc, Life Technologies, Basel, Switzerland) at 0.18 Mio/10 cm dish (wild-type) and 0.35 Mio/10 cm dish (mutants). For immunocytochemistry, wild-type and mutant cells were plated on matrigel-coated chamber slides (Nunc) at 0.02 Mio/2.4 ml and 0.04 Mio/2.4 ml, respectively. Myoblasts were grown to 80% confluency at 33ºC and 5% CO_2 and cells were shifted to fusion media (DMEM supplemented with 2 mM glutamine, 10% fetal bovine serum, 10% horse serum, 2% chick embryo extract and penicillin-streptomycin) at 39ºC, 10% CO_2 to differentiate into myotubes. Both growth and fusion media were replaced every day to ensure good myotube morphology and experiments were conducted on mature myotubes. To induce clustering, myotubes were incubated with 0.5 nM recombinant neural agrin for 15-20 hours (C-Ag$_{12,4,8}$) (Fuhrer et al., 1997). To analyze stability of agrin-induced clusters, myotubes, following overnight agrin treatment, were subsequently washed twice with fusion media and maintained in differentiation media lacking agrin for 3-6 hours. This procedure was shown to be efficient in removing the vast majority of agrin from cells (Mittaud et al., 2004). As shown before (Smith et al., 2001), disassembly of AChR clusters occurs in $src^{-/-};fyn^{-/-}$ myotubes already after 3 hours of agrin withdrawal and more evidently after 5 hours. In parallel wild-type or C2C12 myotubes, little disassembly is visible under these conditions.

AChR precipitation assays and immunoblotting. To examine the association of postsynaptic proteins with the AChR, myotubes were rinsed with ice cold PBS containing 1 mM Na-orthovanadate and 50 mM NaF and extracted at 4ºC in lysis buffer. The lysis buffer contained 1% NP-40 and an excess of protease and phosphatase inhibitors as described earlier (Fuhrer et al., 1999). Lysates were processed and AChRs precipitated using biotinylated α-BT as detailed before (Tox-P) (Mittaud et al., 2001). As a control, an excess of free α-BT (+T) was added to some lysates to judge the specificity of protein association with the AChR. Precipitates were subjected to SDS-PAGE and immunoblotting.

To quantify proteins in total cell extracts, parts of lysates were processed, without precipitation, in parallel by SDS-PAGE and immunoblotting. To ensure proper loading, protein estimations of total lysates were done prior to loading using a standard BCA protein assay kit

(Pierce), and amounts of each protein were normalized to the β-subunit of the AChR on the immunoblot.

In Western blots, α-dystrobrevin-2 was visualized using rabbit polyclonal β1CT-FP antibodies (gift from Dr. Derek J. Blake; University of Oxford). Conditions and antibodies to detect rapsyn, phosphotyrosine, AChR α and β subunit, utrophin and MuSK were as detailed before (Marangi et al., 2001; Moransard et al., 2003). Quantitations of the immunoblots were done by scanning exposed films containing gray, nonsaturated signals with a computerized densitometer (Nikon Scantouch 210) and using the NIH Image J 1.29X software (National Institute of Health, USA). Experiments were repeated at least 5 times to obtain consistent results.

AChR extractability assay. We used a modified version of a sequential extraction procedure detailed before (Borges and Ferns, 2001; Moransard et al., 2003). All steps were carried out on ice if not else specified. 2-3 days old myotubes grown in 10-cm dishes were washed briefly with ice-cold PBS (+ 1 mM Na-Orthovanadate) before adding 1 ml of lysis buffer (30 mM triethanolamine pH 7.5, 50 mM NaCl, 5 mM EDTA, 5 mM EGTA, 50 mM NaF, 1 mM Na-orthovanadate, 1 mM benzamidine, 1mM N-ethylmaleimide, 1 mM Na-tetrathionate, 50 μM phenylarsine oxide, 10 mM p-nitrophenylphosphate, 25 μg/ml aprotinin and leupeptin, 1 mM PMSF) containing a final concentration of Triton X-100 ranging from 0.03% to 0.09%, according to the conditions tested. The exact time for the first extraction was 21 minutes; a timer was started just after addition of lysis buffer to the first plate. Cells were scraped from each plate and the extracts were homogenized by pipetting up and down 10x, then transferred to tubes that were rotated for the rest of the time at 4°C. Extracts were centrifuged for 3 min at 14000 rpm and 4°C in a table eppendorf centrifuge, supernatants were transferred to fresh tubes and called „first extraction". Pellets were resuspended in 1 ml lysis buffer containing 1% Triton X-100 for a total extraction time of exactly 15 min. Again, timer was started after the first resuspension and tubes were rotated together at 4°C for the rest of the time, and finally centrifuged under the same conditions. Supernatants were transferred to fresh tubes and called „second extraction". Both series of tubes were then subjected to AChR-precipitation with biotinylated α-BT, followed by immunoblotting for AChR α as described above.

Immunocytochemical staining procedures and quantitation of clusters. Cultured myotubes were grown in matrigel-coated multiwell chamber slides. Stainings for AChR, α-dystrobrevin-1, utrophin, rapsyn, α-dystroglycan, syntrophin isoforms and phosphotyrosine were all done exactly as described before (Marangi et al., 2001; Moransard et al., 2003). Myotubes were examined at 400-fold magnification in both Rhodamine and Fluroscein channels with a

fluorescence microscope (Axioskop II, Zeiss, Germany). Representative pictures were taken and processed with a cooled digital Camera (Orcacam, Hamamatsu, Japan).

To quantitate clusters, a total of 20 representative pictures per condition were taken from several chamberslides. Clusters of AChR and the respective postsynaptic proteins were counted as done before (Marangi et al., 2001), based on signal intensity (clearly distinguishable from the diffuse background) and the length of the cluster being at least 10 μm. Numbers of clusters per myotubes were calculated independently for the AChR and the postsynaptic marker and averaged. Co-localization of clusters were calculated as the percentage of number of AChR clusters containing the postsynaptic marker protein. Staining experiments were repeated several times to ensure reproducibility.

Results

Role of SFKs: correctly balanced kinase activity is required to maintain adult NMJs in vivo
We addressed the role of SFKs in NMJ stabilization using an in vivo electroporation paradigm in soleus muscle of adult mice. This method allows one to import plasmids into synaptic and extrasynaptic regions of individual myofibers (Kong et al., 2004). Successfully electroporated fibers are identified by nuclear GFP-staining, since a GFP construct containing a nuclear localization signal is co-electroporated (Kong et al., 2004).

We first used a kinase-inactive Src expression construct, Src-AM, in this approach. Src-AM harbors two mutations, K295M and Y527F, which inactivate the kinase activity and the inhibitory C-terminal phosphorylation site, respectively. The resulting kinase-dead molecule preferentially adopts an open conformation and acts strongly in a dominant-negative way (Kaplan et al., 1994; Thomas and Brugge, 1997). Such dominant-negative Src constructs interfere with many members of the Src-family (e.g. Src, Fyn and Yes), not just Src itself. The constructs therefore lead to reduction of cellular SFK function (Twamley-Stein et al., 1993; Roche et al., 1995).

Following electroporation of plasmids expressing siRNA against MuSK, postsynaptic AChR clusters are normal after two weeks but disassembled after 6 weeks (Kong et al., 2004). Apparently, adult NMJs are stabilized, presumably through multiple protein interactions and the cytoskeleton, such that it takes 6 weeks to see disassembly when a critical kinase - MuSK - is inactivated. Since SFKs are also tyrosine kinases, can interact with MuSK and act within the MuSK signaling pathway (Mohamed et al., 2001; Mittaud et al., 2004), we concentrated our analysis to 6 weeks after electroporation of Src-AM. Whole-mount preparations of myofibers were subjected to α-bungarotoxin (α-BT)-rhodamine, neurofilament and synaptophysin staining (in blue) and fluorescence microscopy (Fig. 1). In GFP-positive fibers (expressing Src-AM), AChR clusters often appeared partially disassembled: the typical "pretzel" shapes were disturbed in that they did not form one single continuous structure but contained substantial holes, fragmenting pretzels often into two or more subregions (Fig. 1A, middle). More dramatically, in some GFP-positive fibers NMJs were completely disassembled, so that no pretzels were observed at all but only small fragments of AChR-clusters (Fig. 1A, right). Confocal imaging confirmed these results and allowed, in 3-dimensional reconstruction, to better visualize the disassembly of AChR clusters in fibers expressing GFP and Src-AM (Fig. 1B). We again observed several degrees of fragmentation, ranging from partial (Fig. 1B, middle two columns) to complete disassembly (Fig. 1B, right). As controls, we used GFP-negative fibers in Src-AM

experiments (Fig. 1A) or an empty expression vector lacking the Src-AM insert (Fig. 1B). In both cases, NMJs appeared mostly intact.

Rotation of 3D reconstructions using Imaris software revealed the typical architecture of intact NMJs in muscles electroporated with empty control vector: GFP-labeled synaptic nuclei were properly clustered underneath the AChR-pretzel, and AChRs mostly underneath the nerve (Fig. 1B and 2A-E). This topology was disturbed in fragmented NMJs in fibers expressing Src-AM. Here, remnants of AChR-pretzels were in the same focal plane as the nerve with no preferential labeling underneath it (confirmed by analysis of single confocal stacks; data not shown), such that the nerve was equally visible from a top view and a view from inside the muscle (Fig. 1B and 2F-J). In addition, clusters of synaptic nuclei became dispersed, following the fragmentation of the AChR-pretzels. In fragmented NMJs, we occasionally observed nerve labeling that resembled sprouting (Fig. 1B, middle Src-AM column). We quantitated the proportion of normal, partially and completely disassembled AChR clusters for Src-AM-expressing and control fibers. In the control, most endplates contained intact AChR-pretzels, some scored as partially disassembled clusters but we observed almost no completely disassembled cases (Fig. 2K). In Src-AM-expressing fibers, the proportion of partially and completely disassembled endplates was much higher (Fig. 2K).

We repeated these experiments using another Src mutant, a construct that carried only a single mutation, K295M. This is the classic kinase-inactive, dominant-negative Src form, used most often to investigate the involvement of SFKs in signaling pathways (Kaplan et al., 1994; Roche et al., 1995; Thomas and Brugge, 1997). We observed results very similar to those with Src-AM (Fig. 2L). Taken together, these data demonstrate that normal SFK activity is a requirement to maintain the proper structure of adult NMJs in vivo.

In most cells, SFK activation is under tight regulation by a variety of extracellular signals and intracellular protein interactions (Thomas and Brugge, 1997). Experimentally, reducing or increasing SFK activity can produce changes in downstream signaling pathways (Thomas et al., 1995; Brandt et al., 2002; Kilarski et al., 2003). We therefore addressed whether increased SFK activity, leading to gain of SFK function, would disturb the postsynaptic organization of AChRs. For this purpose, we electroporated a Src construct, Src-Y527F, in which the inhibitory C-terminal phosphorylation site is replaced by phenylalanine. The resulting Src kinase is disinhibited and constitutively activated (Kaplan et al., 1994; Kilarski et al., 2003). In GFP-positive fibers, many AChR structures resembled perforated pretzels, containing holes or broken-up regions, very similar to partially disassembled endplates observed with Src-AM (Fig. 3A). Confocal 3-dimensional imaging illustrated the process of postsynaptic disassembly, revealing that synaptic nuclei were more dispersed, as the AChRs (Fig. 3B). Interestingly, in fibers

expressing Src-Y527F we observed no completely disassembled AChR clusters, unlike for Src-AM. Quantitation showed that Src-Y527F expression strongly increased the proportion of partially disassembled AChR pretzels in comparison to control situations (Fig. 3C).

Taken together, the data demonstrate that proper regulation of kinase activity of SFKs in myofibers is a critical aspect in maintaining a normal morphology of the NMJ. If SFK activity is decreased, due to dominant-negative kinase-dead Src expression, postsynaptic organization is strongly affected, ranging from partial to complete disassembly of AChR-pretzels and alterations in the relative topology of nerve terminals, AChRs and synaptic nuclei. If SFK activity is increased, by expressing overactive Src, the morphology is also disrupted, albeit to a lesser degree.

Expression of dominant-negative Src alters the subsynaptic but not extrasynaptic cytoskeleton and does not cause muscle degeneration

It was important to ascertain that Src-AM electroporation directly affects postsynaptic processes and not global muscle substrates that may indirectly lead to synaptic changes. We focussed on two cytoskeletal elements and known substrates of SFK-activated signaling cascades, F-actin and α-tubulin. In other cells, kinase-dead as well as kinase-overactive Src expression affects their organization (Cox and Maness, 1993; Thomas et al., 1995; Brandt et al., 2002; Kilarski et al., 2003). We stained whole-mount preparations with fluorescent phalloidin to visualize actin filaments and found a transverse pattern throughout myofibers. This is indicative of costameric structures (Rybakova et al., 2000), and there was no difference between Src-AM-expressing and control fibers that had disassembeld and intact NMJs, respectively (Fig 4A). α-tubulin stains revealed typical ring-like structures in the subsynaptic zone of the NMJ, as reported before (Ralston et al., 1999) (Fig. 4B, arrows). Analysis of single confocal sections located the rings subsynaptically underneath AChR clusters (data not shown). These rings often surrounded synaptic nuclei as shown before (Ralston et al., 1999) and as verified in our control experiments using empty vector and GFP (data not shown). Importantly, the rings and the overall intensity of synaptic tubulin staining were much less pronounced at disassembled endplates in fibers expressing Src-AM (Fig. 4B). The irregular extrasynaptic α-tubulin signal showed no difference between Src-AM-epressing and control fibers. These data show cytoskeletal changes at dispersed NMJs but not throughout the muscle fiber, strongly suggesting that Src-AM acts through a specific postsynaptic mechanism to disassemble NMJs.

It was also important to verify that Src-AM does not induce muscle degeneration followed by regeneration, a process that could indirectly contribute to postsynaptic disassembly at affected NMJs. A hallmark of muscle degeneration/regeneration is the appearance of myotubes with

smaller diameter and centrally positioned nuclei (Paoni et al., 2002). We analyzed cross-sections of electroporated muscle by triple-labeling with anti-GFP antibodies, rhodamie-α-BT and DAPI. This allowed to identify muscle fibers, due to diffuse GFP-signal, and to observe the positioning of nuclei within those fibers, since most of the strong GFP signals overlapped with the nuclear DAPI signal (Fig. 4C, D). In myofibers expressing Src-AM or empty control vector, all GFP signals were always at the fiber periphery, never in the center (Fig. 4C). Also in fibers expressing Src-AM and having disassembled NMJs, nuclei were peripheral (Fig. 4D). Finally, we did not observe small diameter myotubes. Thus, electroporation with empty vector or Src-AM does not lead to detectable degeneration and regeneration of muscle, implying that Src-AM expression disrupts the postsynaptic NMJ apparatus by a more direct subsynaptic mechanism.

Mechanism of SFK action: they do not act in recruitment but in stabilization of postsynaptic proteins in clusters

We examined the postsynaptic mode of action of SFKs in stabilizing AChR clusters, by using cultured $src^{-/-};fyn^{-/-}$ myotubes for detailed cell biological and biochemical analysis. These cells are a useful model for postsynaptic stabilization: synapse-promoting factors such as neural agrin or laminin induce normal AChR clustering, but most clusters disassemble when these factors are withdrawn from the cell medium for a few hours, while clusters in wild-type cells remain stable (Smith et al., 2001; Marangi et al., 2002).

We first addressed whether SFKs act in stabilization of agrin-induced AChR clusters by recruiting other proteins into AChR-containing aggregates. We analyzed many UGC components, since this complex plays a central role in postsynaptic stabilization and maturation (Grady et al., 1997; Grady et al., 2000; Jacobson et al., 2001). We treated cultured $src^{-/-};fyn^{-/-}$ myotubes with agrin and examined them by immunocytochemical staining and fluorescence microscopy. Utrophin, α-dystrobrevin, α-dystroglycan, syntrophin, rapsyn and phosphotyrosine-containing proteins were all clustered normally by agrin treatment, and all proteins efficiently colocalized with AChRs (Fig. 5). Recruitment of these proteins into AChR-containing clusters occurs thus independently of Src and Fyn.

We next asked whether SFKs act in stabilizing clusters of postsynaptic proteins, by treating $src^{-/-};fyn^{-/-}$ myotubes with agrin to induce aggregates. Agrin was then withdrawn for 4-5 h to assess the stability of these clusters. Utrophin clusters disappeared rapidly in parallel with AChR aggregates: the number of remaining utrophin clusters was as low as the number of AChR aggregates after 4 h withdrawal, and remaining AChR clusters colocalized efficiently with utrophin (Fig. 6A, B and Supplementary Fig. 1). We observed the same for α-dystrobrevin (Fig. 6C) and rapsyn (Fig. 6D)(see also Supplementary Fig. 1). These data demonstrate that SFKs are

not essential in the formation of clusters of postsynaptic proteins. Rather SFKs are required for stabilization of AChRs and all other proteins examined in co-extensive clusters, illustrating a general importance of SFKs in postsynaptic maintenance by holding together the postsynaptic apparatus.

SFKs maintain agrin-induced AChR-rapsyn interaction

To unravel the mechanisms by which SFKs maintain clusters of AChRs and other postsynaptic proteins, we analyzed AChR-protein interactions biochemically in $src^{-/-};fyn^{-/-}$ myotubes, focusing first on rapsyn. Rapsyn is a key anchor for the AChR in clusters (Gautam et al., 1995) and its interaction with the receptor is highly regulated and increased by agrin (Moransard et al., 2003). Rapsyn exists in free and AChR-bound form (Marangi et al., 2001; Moransard et al., 2003). While intracellular and unclustered surface AChRs interact with some rapsyn, agrin induces increased rapsyn-AChR binding at the plasma membrane, and this increase tightly correlates with clustering and cytoskeletal anchoring. Likewise, synaptic AChRs contain more bound rapsyn than extrasynaptic AChRs in denervated muscle (Moransard et al., 2003). Since increased rapsyn-AChR interaction thus underlies clustering, we analyzed this interaction in cluster formation and stabilization in the absence of Src and Fyn. We treated $src^{-/-};fyn^{-/-}$ myotubes with agrin and then withdrew agrin for 3 or 5 hrs (Fig. 7A). AChRs were precipitated from lysates using biotinylated α-BT and streptavidin-agarose (Tox-P), and AChR-bound rapsyn was visualized by immunoblotting. Interestingly, in untreated $src^{-/-};fyn^{-/-}$ myotubes, α-BT-precipitated AChRs contained in average more associated rapsyn than in wild-type cells (Fig. 7A, B). This interaction was further increased ca. two-fold by agrin treatment, but returned to basal levels within 5 h of agrin withdrawal. In contrast, rapsyn binding to AChR in wild-type cells, increased by agrin to the same relative degree (ca. two-fold) as in the mutant, remained increased even after 5 h withdrawal (Fig. 7A, B). Thus, although AChRs contain in average more associated rapsyn in $src^{-/-};fyn^{-/-}$ myotubes, the agrin-induced increase in the interaction is very unstable in the absence of Src and Fyn.

We previously quantitated the degree of rapsyn co-precipitation with AChRs and found that not every precipitated receptor molecule is associated with one rapsyn molecule (Fuhrer et al., 1999). Other observations suggested that rapsyn exists in an equilibrium between free and AChR-associated state (Marangi et al., 2001; Moransard et al., 2003) and that the average ratio of rapsyn to AChR expression is ca. 1:1 (LaRochelle and Froehner, 1987). The extraction step of our α-BT precipitation of AChRs is likely to break up some AChR-rapsyn-interaction (Fuhrer et al., 1999). For these reasons, the higher basal degree of rapsyn co-precipitation with AChRs in

$src^{-/-};fyn^{-/-}$ myotubes may originate from a weakened cytoskeletal linkage of rapsyn, making its extraction and co-precipitation with the receptor more efficient. Alternatively, rapsyn protein may be present in higher amount in the mutant cells, so that more rapsyn is available to bind the receptor in the absence of Src and Fyn. To distinguish between these two possibilities, we analyzed two aspects of rapsyn in $src^{-/-};fyn^{-/-}$ myotubes.

First, we determined the amount of rapsyn protein in cellular lysates. Using immunoblotting, we observed higher amounts of rapsyn protein per milligram of cellular protein in standard lysates, made with 1% detergent, of $src^{-/-};fyn^{-/-}$ cells as compared to wild-type cells (Fig. 7C and D). In many further extractions using milder and harsher conditions (decreasing or increasing detergent and salt concentrations), we always found similarly elevated rapsyn protein levels in $src^{-/-};fyn^{-/-}$ cells (data not shown). As control, we quantitated the cellular amounts of other postsynaptic proteins, such as utrophin, MuSK and α-dystrobrevin. We observed no significant difference in these proteins between mutant and wild-type cells (data not shown), suggesting that the effect of Src and Fyn on rapsyn levels is specific.

Second, we measured the relative strength of cytoskeletal rapsyn interaction. We performed extraction experiments similar to those described in detail for AChRs in Figure 9, employing low and high detergent concentrations. By immunoblotting we determined the proportion of rapsyn in each of these extractions. The proportion of rapsyn in low versus high detergent extractions was the same for $src^{-/-};fyn^{-/-}$ and wild-type myotubes (data not shown), showing that the cytoskeletal link of rapsyn is unchanged in the mutant.

Taken together, these data, combined with earlier observations (Marangi et al., 2001; Moransard et al., 2003), strongly imply that since $src^{-/-};fyn^{-/-}$ myotubes contain elevated levels of rapsyn protein, rapsyn associates to a higher overall degree with the AChR. But the agrin-induced rapsyn interaction is very unstable following agrin withdrawal from mutant cells. This instability parallels the concomitant disappearance of AChR and rapsyn clusters (Fig. 6). Thus stabilization of rapsyn-AChR interaction appears as primary mechanism by which SFKs hold together the postsynaptic apparatus.

SFKs maintain AChR-dystrobrevin interaction and AChR phosphorylation

In the process of clustering, agrin increases some but not all interactions of AChRs with other proteins (Fuhrer et al., 1999). We investigated whether α-dystrobrevin, a UGC component essential for stabilization of the postsynaptic membrane and AChR aggregates (Grady et al., 2000), increasingly associates with AChRs following agrin treatment and withdrawal. We focused on the α-dystrobrevin-2 isoform, since our available antibodies best allowed detection of

this form. Precipitation with α-BT and α-dystrobrevin-2 immunoblotting revealed that agrin induces increased binding of α-dystrobrevin-2 to AChRs in both wild-type and $src^{-/-};fyn^{-/-}$ myotubes (Fig. 8A). Following withdrawal of agrin, however, less α-dystrobrevin-2 remained bound to the receptor in the mutant as compared to wild-type cells (Fig. 8A), showing that Src and Fyn are required for optimal stabilization of AChR-UGC interaction. This parallels the stabilization by SFKs of AChR-rapsyn interaction, consistent with the idea that rapsyn is a linker between AChR and the UGC (Apel et al., 1995; Cartaud et al., 1998; Bartoli et al., 2001).

Phosphorylation of the AChR β subunit is a key event in agrin signaling and important for efficient clustering and cytoskeletal linkage of the receptor (Borges and Ferns, 2001). Agrin-induced AChR β phosphorylation is an early step in agrin signaling and precedes receptor clustering, similar to agrin-triggered rapsyn-AChR interaction (Ferns et al., 1996; Moransard et al., 2003). We examined whether SFKs are required to maintain this phosphorylation in the process of cluster stabilization. Precipitation with biotin-α-BT and immunoblotting with anti-phosphoytrosine showed that agrin treatment caused normal β phosphorylation in $src^{-/-};fyn^{-/-}$ myotubes, as described previously (Smith et al., 2001). But following agrin withdrawal, this phosphorylation was unstable and disappeared much faster than in wild-type cells (Fig. 8B). While in the wild-type, significant β phosphorylation persisted 5 h after agrin withdrawal, β phosphorylation was already down at basal levels after 3 h in $src^{-/-};fyn^{-/-}$ myotubes (Fig. 8B). We thus estimate the half-life time ($t_{1/2}$) of β phosphorylation to be about 4 h in the wild-type but less than 90 min in the mutant. Since AChRs can be direct substrates for SFKs (Swope and Huganir, 1993; Fuhrer and Hall, 1996; Mohamed et al., 2001; Mittaud et al., 2004), these data strongly imply that SFK activity is required to maintain phosphorylation of the AChR, and that the receptor is a direct substrate for SFKs at that stage.

The correlation between loss of AChR phosphorylation and AChR-rapsyn binding following agrin removal raises the possibility that β phosphorylation may regulate rapsyn interaction. Collectively, the sum of our data on $src^{-/-};fyn^{-/-}$ myotubes up to this point suggests that SFK-mediated stabilization of AChR phosphorylation and of AChR association with rapsyn and dystrobrevin form a core mechanism by which SFKs hold together proteins of the postsynaptic apparatus.

The overall link of AChRs to the cytoskeleton is weak in $src^{-/-};fyn^{-/-}$ myotubes but still strengthened by agrin

In addition to changes at the level of AChR clusters, the alterations in postsynaptic architecture in Src-AM-expressing myofibers in vivo suggest that the postsynaptic cytoskeleton (as shown for

α-tubulin in Fig. 4B) and its protein interactions may be altered upon loss of SFK function. To further test this hypothesis, we analyzed the role of SFKs in interactions of the AChR with the cytoskeleton. We quantitated the AChR extractability in $src^{-/-};fyn^{-/-}$ myotubes, by applying a sequential detergent extractability protocol in which a first extraction in low detergent is followed by a second extraction in higher detergent concentration. From each extraction, we precipitated AChRs using biotin-α-BT, visualized them in Western blots, and calculated the receptor distribution between first and second extraction, using increasing detergent concentrations in the first extraction (Fig. 9A, B). Such methods are established measures for the relative strength of the interaction of the AChR to the cytoskeleton (Borges and Ferns, 2001; Moransard et al., 2003). We found that in wild-type myotubes, AChR started to become efficiently solubilized in the first extraction when the concentration of first detergent was 0.06% Triton X-100 (Fig. 9A). At lower Triton X-100 concentrations in the first extraction, receptors appeared in the second extraction, while at higher concentrations, AChRs participated into the first extraction (Fig. 9A). In contrast, in $src^{-/-};fyn^{-/-}$ myotubes, a concentration of 0.04% Triton X-100 was sufficient to efficiently solubilize AChRs in the first extraction (Fig. 9B). These data reveal that the overall basal cytoskeletal link of the AChR is weakened in the absence of Src and Fyn.

Agrin treatment is known to strengthen the AChR-cytoskeletal link in the process of cluster formation (Wallace, 1992, 1995; Borges and Ferns, 2001; Moransard et al., 2003). This is manifested as a decrease of solubilized and precipitated AChR in the first extraction and an increase of receptor in the second extraction (Borges and Ferns, 2001; Moransard et al., 2003). Likewise, AChRs increasingly become cytoskeletally anchored at developing NMJs in vivo (Dennis, 1981; Slater, 1982). We analyzed whether agrin affects the weak overall cytoskeletal interaction of the AChR in $src^{-/-};fyn^{-/-}$ myotubes, by quantitating the relative amounts of AChRs in the first and second extraction in agrin-treated and untreated cells. Agrin caused a shift of receptors from the first (0.05% Triton X-100) to the second (1% Triton X-100) extraction in $src^{-/-};fyn^{-/-}$ myotubes (Fig. 9C and D), similar to results previously seen in wild-type cells (Borges and Ferns, 2001; Moransard et al., 2003). The percentage of agrin-induced decrease of AChR precipitated from the first extraction was identical between C2 myotubes, wild-type myotubes and $src^{-/-};fyn^{-/-}$ myotubes (Fig. 9E).

Together, these results show that while the overall basal cytoskeletal linkage of AChRs is weaker in the absence of Src and Fyn, agrin treatment still strengthens this link. This is consistent with the normal phosphorylation and cluster formation of AChRs in agrin-treated $src^{-/-};fyn^{-/-}$ myotubes and the decreased stability of such clusters following removal of agrin (Smith

et al., 2001). Most likely, the agrin-induced strengthening of the AChR cytoskeletal link in mutant cells originates from linkage of the receptor to the UGC, since AChR-dystrobrevin-interactions are normally induced by agrin in these cells (Fig. 8A), and since the UGC interacts with F-actin (Winder et al., 1995).

Discussion

Our data reveal that SFKs are key players in the pathways that stabilize the postsynaptic apparatus of the NMJ in vivo. They act by holding postsynaptic proteins together in clusters through stabilization of rapsyn-AChR interaction and AChR phosphorylation. In addition, they control rapsyn protein levels and AChR-cytoskeletal linkage.

SFKs hold together the postsynaptic apparatus

Interference with SFK function causes complex alterations at adult NMJs. Upon Src-AM expression, AChR pretzels fragment and attach to the nerve in the same focal plane (not underneath it), subsynaptic α-tubulin organization is disturbed, synaptic nuclei become more dispersed and nerves occasionally sprout. These changes originate from Src-AM expression in muscle, acting specifically on postsynaptic mechanisms: GFP-positive nuclei were only seen in myofibers and never in other cells (e.g. Schwann cells), confirmed by 3D-reconstruction (G. Sadasivam and C. Fuhrer, unpublished observations), and costameric F-actin organization along myofibers was not affected. Nerve sprouting is in accordance with studies showing that postsynaptic disturbance affects the nerve, leading to sprouting or, as is the case in rapsyn- or MuSK-deficient mice, extensive nerve growth (Gautam et al., 1995; DeChiara et al., 1996; Kong et al., 2004).

The effects of Src-Y527F expression are similar, illustrating that correctly balanced SFK activity is important to maintain the postsynaptic apparatus in vivo. Consistent with this, reducing or increasing SFK activity experimentally leads to changes in downstream pathways and affects cytoskeletal organization, for example actin fibers, in other cell types (Thomas et al., 1995; Brandt et al., 2002; Kilarski et al., 2003).

We investigated the consequences of reduced SFK function using $src^{-/-};fyn^{-/-}$ myotubes, where agrin normally recruited postsynaptic proteins into AChR-containing clusters. This parallels the normal development, until birth, of endplates in $src^{-/-};fyn^{-/-}$ mice (Smith et al., 2001). But after agrin removal from $src^{-/-};fyn^{-/-}$ myotubes, clusters of UGC and rapsyn disintegrated in parallel with AChRs. Thus Src and Fyn hold together the postsynaptic apparatus, consistent with AChR pretzel disassembly in Src-AM-expressing myofibers.

SFKs maintain AChR-rapsyn interaction and AChR phosphorylation

In parallel with unstable clusters, AChR-protein interactions are unstable in $src^{-/-};fyn^{-/-}$ myotubes, and the key compromised interaction is that between AChRs and rapsyn. Agrin-induced increase in AChR-rapsyn interaction correlates highly with clustering (Moransard et al.,

2003), and increased rapsyn binding slows metabolic AChR turnover (Gervasio and Phillips, 2005). AChRs and rapsyn are the most abundant postsynaptic components. Occasionally, AChR-rapsyn complexes are linked to the UGC through dystroglycan, giving rise to a corral model in which postsynaptic proteins such as the UGC are held together through many AChR-rapsyn complexes (Apel and Merlie, 1995)(Fig. 10). If the rapsyn-AChR interaction breaks, AChR-UGC interactions and clusters of all postsynaptic proteins are expected to disintegrate, and this is what our data on *src-/-;fyn-/-* myotubes indeed show. Thus the primary mode of SFK action in postsynaptic stabilization is to maintain the AChR interaction with its anchor rapsyn (Fig. 10, pathway 1).

SFKs also maintain AChR phosphorylation. Phosphorylation of AChR β, required for efficient AChR cytoskeletal linkage and clustering (Borges and Ferns, 2001), can directly be mediated by SFKs, at least in vitro (Swope and Huganir, 1993; Fuhrer and Hall, 1996). Upon agrin stimulation of myotubes, however, SFKs only act in the initial phase, are later compensated by Abl kinases and not necessary for cluster formation (Mittaud et al., 2004). We now find that Src and Fyn are required to maintain β phosphorylation, and this most likely reflects direct phosphorylation. Loss of β phosphorylation may lead to weaker AChR-cytoskeletal linkage, but we were not able to reliably quantify AChR-extractability after agrin withdrawal due to variation between experiments (R. Willmann and C. Fuhrer, unpublished observations).

In *src-/-;fyn-/-* myotubes, loss of β phosphorylation after agrin withdrawal is paralleled by loss of AChR-rapsyn interaction. Additional experiments have further corroborated a tight correlation: while agrin induces pronounced β phosphorylation and rapsyn-binding in C2 myotubes, pervanadate treatment causes stronger β phosphorylation and stronger rapsyn binding, revealing a linear relationship between the two events (M. Moransard and C. Fuhrer, unpublished observations). Furthermore, the time course of agrin-induced β phosphorylation exactly parallels that of AChR-rapsyn binding (M. Moransard and C. Fuhrer, unpublished observations). Thus, increased AChR-rapsyn binding may occur through β phosphorylation, via direct protein interaction or through an intermediate linker (Fig. 10, pathway 1). Consequently, loss of β phosphorylation may diminish AChR-rapsyn interaction, causing postsynaptic disassembly. The proposal that rapsyn binds AChRs in several ways - in basal state independent of AChR phosphorylation but after agrin addition through increased receptor phosphorylation (Fig. 10) - is consistent with findings from heterologous cells. Here, rapsyn directly or indirectly interacts with AChRs in multiple ways through association with all receptor subunits (Maimone and Merlie, 1993; Maimone and Enigk, 1999; Bartoli et al., 2001; Huebsch and Maimone, 2003).

More surprisingly, SFKs repress the amount of rapsyn protein (Fig. 10, pathway 2). Correct expression level of rapsyn is important, as its overexpression reduces AChR clustering in myotubes (Yoshihara and Hall, 1993; Han et al., 1999). We did not investigate whether alterations in rapsyn synthesis, degradation or turnover cause the increase in overall rapsyn protein. More importantly, we found that rapsyn's own cytoskeletal link is unaffected by Src and Fyn. In heterologous cells, SFKs form a complex with rapsyn and rapsyn triggers their kinase activity, leading to AChR phosphorylation (Mohamed and Swope, 1999). In myotubes, rapsyn is required for agrin-induced activity of SFKs, implying an interaction between rapsyn and SFKs (Mittaud et al., 2001). Thus SFK and rapsyn seem to be engaged in mutual control, leading to correct rapsyn protein levels and SFK activity. Fine-tuning of such interactions and activities may be important for correct protein interactions in building up and stabilizing the postsynaptic apparatus, and for appropriate linkage of associated signaling pathways.

SFKs control AChR-cytoskeletal interactions

Unstability of AChR-protein interactions is sufficient to explain the disintegration of postsynaptic protein clusters but may not account for all postsynaptic changes observed in vivo upon Src-AM expression. Changes in nerve-AChR topology and synaptic nuclei positioning are likely to reflect additional changes in the postsynaptic cytoskeleton as illustrated by loss of synaptic α-tubulin rings. Indeed, cytoskeletal linkage of the AChR is weaker in $src^{-/-};fyn^{-/-}$ myotubes, yet strengthened by agrin treatment. One candidate mechanism to explain this observation is the UGC and its interaction with F-actin (Winder et al., 1995). We do not think that the higher rapsyn amount in $src^{-/-};fyn^{-/-}$ cells saturates rapsyn binding sites on AChRs or β-dystroglycan, thereby disturbing AChR-F-actin linkage, since the UGC component dystrobrevin associates normally with AChRs in the mutant cells (Fig. 8A). This leads to the conclusion that another mechanism, potentially involving microtubular organization, accounts for the weaker basal cytoskeletal link of the AChR in $src^{-/-};fyn^{-/-}$ myotubes. Such a mechanism may not involve rapsyn as a linker, because rapsyn's own cytoskeletal interaction is normal in the mutant cells. More likely, the AChR interacts directly or indirectly with other elements of the cytoskeleton through a novel pathway, before and after agrin treatment, and such linkage depends on Src and Fyn (Fig. 10, putative pathway 3). Agrin-triggered strengthening of the overall AChR-cytoskeletal link may stem from agrin-induced AChR-UGC interaction, as agrin induces normal AChR-dystrobrevin association, in mutant and wild-type myotubes. In such a manner, normal AChR-UGC association in combination with defects in a putative additional cytoskeletal pathway provides an explanation for the observed alteration in overall AChR extractability in SFK-defective cells.

The intermediate elements in the putative SFK-mediated cytoskeletal pathway remain to be identified. Candidates are known SFK-substrates involved in cytoskeleton dynamics, such as cortactin and WASP (both regulating the Arp2/3 complex) (Daly, 2004; Martinez-Quiles et al., 2004) or p190RhoGAP (influencing Rho GTPase activity) (Chang et al., 1995), which all ultimately regulate F-actin assembly. Reduction or increase in SFK activity affects the organization of actin fibers in other cell types (Thomas et al., 1995; Brandt et al., 2002; Kilarski et al., 2003), consistent with our finding that both Src-AM and Src-Y527F expression disassembles AChR pretzels in vivo. Rho, along with Rac and Cdc42, is already known to play a role in AChR cluster formation in cultured myotubes (Weston et al., 2000; Weston et al., 2003). SFKs also influence the tubulin network (Cox and Maness, 1993), and we have observed changes in synaptic tubulin organization following Src-AM expression.

It remains to be investigated what other connections between SFKs and the cytoskeleton and its regulators exist at the NMJ, affecting postsynaptic stability. As balanced SFK activity is important (Fig. 1-3), SFKs may be counteracted by tyrosine phosphatases. Phosphatase activity dissolves AChR hot spots in cultured Xenopus myocytes, and some of this activity is triggered by agrin application (Madhavan et al., 2005). The phosphatase Shp-2 is a possible candidate, as blocking Shp-2 increases spontaneous AChR clustering (Madhavan et al., 2005). The balance between SFKs and phosphatases offers a fine-tuning system to shape the postsynapse. It will be interesting to assess the role of such a system in vivo, also in the first weeks of postnatal NMJ development, when synapse elimination occurs. In this process, AChR regions can be selectively destabilized paralleled by nerve withdrawal (Lichtman and Colman, 2000), and a tyrosine kinase-phosphatase regulation is an attractive candidate mechanism.

Figure Legends

Figure 1. Electroporation of kinase-inactive Src-AM into soleus muscle leads to disassembly of NMJs. Muscles were electroporated in vivo with a mixture of Src-AM and NLS-GFP or empty control vector and NLS-GFP. 6 weeks later, muscles were dissected and whole mounts of fibers stained with α-BT-rhodamine and a mixture of neurofilament (NF) and synaptophysin (Syn) antibodies (in blue). (A) Conventional microscopy shows that in GFP-positive fibers NMJs are partially (middle, arrow) or completely (right) disassembled, while GFP-negative fibers show intact NMJs (left, and arrowhead in middle). (B) Confocal microscopy with 3D reconstruction to visualize the degree of NMJ disassembly and the topology of nerve, AChRs and synaptic myonuclei. Control vector electroporation leaves NMJs intact (left), while Src-AM electroporation disassembles NMJs in GFP-positive (arrows in middle columns) but not GFP-negative fibers (arrowheads in middle columns). Disassembly ranges from partial (middle columns) to complete (right). Occasionally, nerves of disassembled NMJs show sprouting as indicated by the small arrowheads. Clusters of synaptic nuclei are less dense in disassembled NMJs, and the topology of nerve versus AChRs is disturbed.

Figure 2. 3-dimensional rotation and quantitation of intact and disassembled endplates of muscle fibers expressing control plasmid or kinase-inactive Src. (A-J) 3D-reconstructions as shown in Fig. 1B were rotated around the x-axis to illustrate the relative positioning of nerve, AChR clusters and GFP-stained nuclei. (K and L) In experiments as described in Fig. 1, the degree of NMJ disassembly was scored as detailed in Materials and Methods. Control fibers score mostly as intact endplates with some partial and no complete disassembly. Fibers expressing Src-AM (K) or Src-K295M (L) show a high percentage of complete and partial disassembly as compared to control. Disassembly is quantified as percentage of all endplates analyzed within the control, Src-AM and Src-K295M groups. 50 endplates were analyzed for each group.

Figure 3. Electroporation of constitutively active Src-Y527F leads to partial disassembly of NMJs in vivo. Experiments were performed as for Figure 1 and 2. (A) Conventional microscopy shows that upon Src-Y527 electroporation, NMJs disassemble partially in GFP-positive fibers but not in GFP-negative fibers or in control muscles that were not electroporated. (B) Confocal analysis illustrates the partial disassembly of an endplate, displaying large holes between AChR pretzel fragments. Nerves and synaptic nuclei are arranged accordingly. (C)

Quantitation of 30 Src-Y527F and 30 control situations shows that Src-Y527F expression increases partial disassembly without leading to complete disassembly.

Figure 4. Electroporation of Src-AM causes specific cytoskeletal changes at the postsynapse and does not induce muscle degeneration/regeneration. (A, B) Muscles were electroporated with Src-AM and NLS-GFP, and whole mounts stained with rhodamine-α-BT and Alexa 350-coupled phalloidin (to visualize actin filaments)(A; blue) or antibodies against α-tubulin (B; pink). The organization of F-actin in costameric structures along myofibers is not affected in Src-AM-expressing, GFP-positive fibers in which NMJs are disassembled (A). Subsynaptic α-tubulin is organized in ring-like structures at intact NMJs (arrows in B), and this arrangement is disturbed at disassembled NMJs in GFP-positive fibers. (C) Muscles were electroporated with Src-AM and NLS-GFP, or empty control vector and NLS-GFP. Muscles were first processed and fixed as for whole-mount analysis, but then embedded, cryosectioned, and stained with anti-GFP antibodies and DAPI as described in Materials and Methods. Muscles fibers are visible due to low-intensity diffuse GFP-staining. In both Src-AM and vector samples, strong GFP signals are always at the fiber periphery and mostly colocalize with DAPI, identifying them as peripheral nuclei (arrows). Thus Src-AM does not lead to centrally positioned nuclei, excluding the presence of myotubes and degeneration/regeneration. (D) Samples as in C were additionally stained with rodamine-α-BT. Fibers lacking nuclear GFP-signal show intact AChR clusters (asterisks), while a fiber with disassembled AChR clusters (arrowhead) displays peripheral nuclei (arrows).

Figure 5. Agrin induces co-clustering of postsynaptic proteins with AChRs in *src^{-/-};fyn^{-/-}* myotubes. (A) Cells were incubated with 0.5 nM agrin overnight and double-labelled with rhodamine-α-BT (AChR) and antibodies recognizing α-dystrobrevin-1 (α-DB), utrophin (Utro), rapsyn (Rap), α-dystroglycan (α-DG), syntrophin isoforms (Syntro) or phosphotyrosine (PTyr), followed by FITC-coupled secondary antibodies. Wild-type and *src^{-/-};fyn^{-/-}* myotubes show identical co-clustering of AChRs with the respective postsynaptic proteins. Scale bar = 10 μm. (B) Clusters of AChRs and postsynaptic proteins were counted in agrin-treated (ag) and untreated (no ag) cells. (C) Protein colocalization is expressed as % of AChR clusters that contain the respective postsynaptic protein in agrin-treated cells. „No ag" shows the average of colocalization of each marker with AChRs in non agrin-treated cells. Values are mean ± SEM, from 20 pictures for each marker and condition.

Figure 6. Src and Fyn are required to stabilize postsynaptic protein clusters along with AChR clusters. Cells were treated overnight with 0.5 nM agrin to induce protein clustering. For studying cluster maintenance, agrin was then withdrawn from cultures for 4-5 hrs (wd 4h, wd 5h). (A) Cells were labelled with rhodamine-α-BT (AChR), showing that 5 hrs of withdrawal causes pronounced AChR cluster disassembly in $src^{-/-};fyn^{-/-}$ but not wild-type myotubes. Cells were double-labelled with rhodamine-α-BT (AChR) and antibodies recognizing utrophin (B), α-dystrobrevin-1 (C), or rapsyn (D), followed by FITC-coupled secondary antibodies. Illustrative pictures of clusters and their disassembly are shown in Supplementary Fig. 1. Quantitation (left) shows that clusters of these postsynaptic proteins disappear in parallel with AChRs upon agrin withdrawal. Colocalization (right) indicates % of AChR clusters that contain the respective postsynaptic protein, in the case of agrin withdrawal for remaining AChR clusters. Values are mean ± SEM, from 20 pictures for each marker and condition.

Figure 7. SFKs maintain AChR-rapsyn interaction and negatively regulate rapsyn protein levels. (A) Cells were treated overnight with 0.5 nM agrin followed by withdrawal (wd) as indicated. AChRs were precipitated from lysates using α-BT-biotin and streptavidin-agarose (Tox-P), and associated rapsyn was detected by Western blotting. As control, an excess (10 μM) of free soluble toxin (+T) was added to some lysates. In the bottom part, the blots were stripped and reprobed for the AChR β subunits with mAb 124. (B) Experiments were quantitated by densitometric scanning. Rapsyn signals were divided through AChR β signals to ensure equal loading. The graph indicates the % of rapsyn associated with AChR, with wild-type cells not treated with agrin set to 100%. Untreated $src^{-/-};fyn^{-/-}$ myotubes show an increased rapsyn association (ca. 2-fold) with the AChR. Agrin further increases this interaction about 2-fold, similarly to wild-type cells. In $src^{-/-};fyn^{-/-}$ myotubes the agrin-induced increase in rapsyn-AChR interaction decreases after agrin withdrawal but remains more stable in the wild-type. Data represent mean ± SEM of at least 5 experiments. *$p<0.05$, **$p<0.01$, ***$p<0.001$, by unpaired Student's t-tests (n.s., not significant). (C) Protein-matched aliquots of wild-type and $src^{-/-};fyn^{-/-}$ myotube lysates were analyzed by immunoblotting using antibodies against rapsyn (Rap-1) and AChR β subunits (mAb 124). (D) Quantitation shows that the level of rapsyn protein (determined as rapsyn/AChRβ) is two-fold higher in mutant cells.

Figure 8. In $src^{-/-};fyn^{-/-}$ myotubes, AChR-dystrobrevin association and phosphorylation of AChR β subunits are unstable after agrin withdrawal. Agrin was added overnight, cells were washed, and incubated in withdrawal medium (wd) lacking agrin for 3 or 5 hours. AChRs were

25

precipitated with α-BT and subjected to immunoblotting using antibodies against α-dystrobrevin-2 (A) or against phosphotyrosine (B). Blots were stripped and reprobed for AChR α subunits as control. (A) Association of AChRs with α-dystrobrevin is increased by agrin in both wild-type and mutant cells. After 5 hrs agrin withdrawal, the association is much weaker in the mutant than in the wild-type. (B) In mutant cells, phosphorylation of AChR β subunits - detected based on molecular weight and comparison to parallel AChR β immunoblots (not shown) - is normally induced by agrin but rapidly decreases after withdrawal. Quantitation of the phospho-AChR β signal by densitometric scanning, normalized for AChR α, shows a significant decrease in the mutant but not in the wild-type upon agrin withdrawal (mean ± SEM from at least 5 experiments; ***p=0.003; *p=0.018; n.s.: not significant; by unpaired Student's t-tests).

Figure 9. The overall basal cytoskeletal link of AChRs is weakened in *src⁻/⁻;fyn⁻/⁻* myotubes but still strengthened by agrin treatment. Wild-type (A) or *src⁻/⁻;fyn⁻/⁻* myotubes (B) were subjected to a first extraction in a buffer containing a low detergent concentration, ranging from 0.03 to 0.09% Triton X-100 as indicated. Insoluble materials (pellets) were subjected to a second extraction, using 1% Triton X-100. AChRs were precipitated from the soluble low- and high-detergent fractions using α-BT and visualized by anti-AChR α subunit-antibodies in immunoblots. AChR extraction was quantified by densitometric scanning, and AChR signals are shown as % of the sum of both extractions (low + high detergent). Values are mean ± SEM from at least 5 experiments. For wild-type cells, 0.06% detergent extracts about half of the total AChRs, while for *src⁻/⁻;fyn⁻/⁻* myotubes only 0.04% detergent are required to achieve the same, indicating that in the mutant the AChR extractability is higher and thus the cytoskeletal link weaker. (C) Mutant cells were incubated overnight with agrin to induce AChR cluster formation. AChRs were first extracted with 0.05% and then with 1% detergent as described above, and visualized by α-BT precipitation and AChR α immunoblotting. Agrin causes decreased AChR extractability, indicating stronger cytoskeletal linkage, because less AChRs are found in the first extraction and more in the second. (D) Quantitation of experiments as in (C) shows a significant agrin-induced decrease of AChRs in the first extraction and a significant increase in the second extraction. Values are mean ± SEM from 5 experiments, *p=0.03, by unpaired Student's t-tests. (E) Sequential extraction as in (C) was performed for wild-type and C2C12 myotubes, using 0.06% Triton X-100 in the first extraction and 1% in the second. The % of decrease of AChRs in the first extraction, induced by agrin, was quantitated from 5 experiments and is the same, ca. 30-40%, as for *src⁻/⁻;fyn⁻/⁻* myotubes. Thus while the overall cytoskeletal link is weaker in *src⁻/⁻;fyn⁻*

$^{/-}$ myotubes, the agrin-induced strengthening of this link is comparable to wild-type and C2C12 cells.

Figure 10. Model of SFK action in stabilization of the postsynaptic apparatus. Unclustered proteins such as rapsyn (rap) are in equilibrium between free and complexed form, indicated by double arrows. Agrin increases AChR-protein interactions in the process of clustering. SFKs act in postsynaptic stabilization by maintaining the AChR-rapsyn interaction (pathway 1). As rapsyn and AChRs are the most abundant postsynaptic proteins, their interaction plays a core role and holds the postsynaptic apparatus together. This may occur through AChR β phosphorylation (p), which is maintained by SFKs (pathway 1). SFKs also negatively control the overall amount of rapsyn protein (pathway 2). In the absence of Src and Fyn, rapsyn amounts are high and may start saturating binding sites on β-dystroglycan (β-DG) and the AChR, although AChR-dystrobrevin interactions appear normal. SFKs may control another cytoskeletal link (cyto) of the AChR, independent of rapsyn as a linker (hypothetical pathway 3). This would explain the observed weak overall AChR-cytoskeletal linkage in *src$^{-/-}$;fyn$^{-/-}$* myotubes, which is still strengthened upon agrin treatment due to AChR-UGC association. Utro, utrophin; DB, α-dystrobrevin.

Supplementary Figure 1. Src and Fyn are required to stabilize clusters of α-dystrobrevin, rapsyn and utrophin along with AChR clusters. Myotubes were incubated overnight with 0.5 nM agrin following which agrin was withdrawn for 5 h. Cells were double labeled for the AChR with α-BT-rhodamine and for the respective postsynaptic proteins. In *src$^{-/-}$;fyn$^{-/-}$* myotubes clusters of α-dystrobrevin-1 (α-DB), rapsyn (Rap), and utrophin (Utro) disperse in parallel with the AChR clusters. In wild-type cells clusters of AChRs and postsynaptic proteins remain stable.

References

Apel ED, Merlie JP (1995) Assembly of the postsynaptic apparatus. Curr Opin Neurobiol 5:62-67.

Apel ED, Roberds SL, Campbell KP, Merlie JP (1995) Rapsyn may function as a link between the acetylcholine receptor and the agrin-binding dystrophin-associated glycoprotein complex. Neuron 15:115-126.

Bartoli M, Ramarao MK, Cohen JB (2001) Interactions of the rapsyn RING-H2 domain with dystroglycan. J Biol Chem 276:24911-24917.

Bezakova G, Ruegg MA (2003) New insights into the roles of agrin. Nat Rev Mol Cell Biol 4:295-308.

Borges LS, Ferns M (2001) Agrin-induced phosphorylation of the acetylcholine receptor regulates cytoskeletal anchoring and clustering. J Cell Biol 153:1-12.

Brandt D, Gimona M, Hillmann M, Haller H, Mischak H (2002) Protein kinase C induces actin reorganization via a Src- and Rho-dependent pathway. J Biol Chem 277:20903-20910.

Cartaud A, Coutant S, Petrucci TC, Cartaud J (1998) Evidence for in situ and in vitro association between beta-dystroglycan and the subsynaptic 43K rapsyn protein. Consequence for acetylcholine receptor clustering at the synapse. J Biol Chem 273:11321-11326.

Chang JH, Gill S, Settleman J, Parsons SJ (1995) c-Src regulates the simultaneous rearrangement of actin cytoskeleton, p190RhoGAP, and p120RasGAP following epidermal growth factor stimulation. J Cell Biol 130:355-368.

Cox ME, Maness PF (1993) Tyrosine phosphorylation of alpha-tubulin is an early response to NGF and pp60v-src in PC12 cells. J Mol Neurosci 4:63-72.

Daly RJ (2004) Cortactin signalling and dynamic actin networks. Biochem J 382:13-25.

DeChiara TM, Bowen DC, Valenzuela DM, Simmons MV, Poueymirou WT, Thomas S, Kinetz E, Compton DL, Rojas E, Park JS, Smith C, DiStefano PS, Glass DJ, Burden SJ, Yancopoulos GD (1996) The receptor tyrosine kinase MuSK is required for neuromuscular junction formation in vivo. Cell 85:501-512.

Dennis MJ (1981) Development of the neuromuscular junction: inductive interactions between cells. Annu Rev Neurosci 4:43-68.

Ferns M, Deiner M, Hall Z (1996) Agrin-induced acetylcholine receptor clustering in mammalian muscle requires tyrosine phosphorylation. J Cell Biol 132:937-944.

Finn AJ, Feng G, Pendergast AM (2003) Postsynaptic requirement for Abl kinases in assembly of the neuromuscular junction. Nat Neurosci 6:717-723.

Fuhrer C, Hall ZW (1996) Functional interaction of Src family kinases with the acetylcholine receptor in C2 myotubes. J Biol Chem 271:32474-32481.

Fuhrer C, Sugiyama JE, Taylor RG, Hall ZW (1997) Association of muscle-specific kinase MuSK with the acetylcholine receptor in mammalian muscle. Embo J 16:4951-4960.

Fuhrer C, Gautam M, Sugiyama JE, Hall ZW (1999) Roles of rapsyn and agrin in interaction of postsynaptic proteins with acetylcholine receptors. J Neurosci 19:6405-6416.

Gautam M, Noakes PG, Mudd J, Nichol M, Chu GC, Sanes JR, Merlie JP (1995) Failure of postsynaptic specialization to develop at neuromuscular junctions of rapsyn-deficient mice. Nature 377:232-236.

Gervasio OL, Phillips WD (2005) Increased ratio of rapsyn to ACh receptor stabilizes postsynaptic receptors at the mouse neuromuscular synapse. J Physiol 562:673-685.

Grady RM, Teng H, Nichol MC, Cunningham JC, Wilkinson RS, Sanes JR (1997) Skeletal and cardiac myopathies in mice lacking utrophin and dystrophin: a model for Duchenne muscular dystrophy. Cell 90:729-738.

Grady RM, Zhou H, Cunningham JM, Henry MD, Campbell KP, Sanes JR (2000) Maturation and maintenance of the neuromuscular synapse: genetic evidence for roles of the dystrophin--glycoprotein complex. Neuron 25:279-293.

Han H, Noakes PG, Phillips WD (1999) Overexpression of rapsyn inhibits agrin-induced acetylcholine receptor clustering in muscle cells. J Neurocytol 28:763-775.

Huebsch KA, Maimone MM (2003) Rapsyn-mediated clustering of acetylcholine receptor subunits requires the major cytoplasmic loop of the receptor subunits. J Neurobiol 54:486-501.

Jacobson C, Cote PD, Rossi SG, Rotundo RL, Carbonetto S (2001) The dystroglycan complex is necessary for stabilization of acetylcholine receptor clusters at neuromuscular junctions and formation of the synaptic basement membrane. J Cell Biol 152:435-450.

Kaplan KB, Bibbins KB, Swedlow JR, Arnaud M, Morgan DO, Varmus HE (1994) Association of the amino-terminal half of c-Src with focal adhesions alters their properties and is regulated by phosphorylation of tyrosine 527. Embo J 13:4745-4756.

Kilarski WW, Jura N, Gerwins P (2003) Inactivation of Src family kinases inhibits angiogenesis in vivo: implications for a mechanism involving organization of the actin cytoskeleton. Exp Cell Res 291:70-82.

Kong XC, Barzaghi P, Ruegg MA (2004) Inhibition of synapse assembly in mammalian muscle in vivo by RNA interference. EMBO Rep 5:183-188.

LaRochelle WJ, Froehner SC (1987) Comparison of the postsynaptic 43-kDa protein from muscle cells that differ in acetylcholine receptor clustering activity. J Biol Chem 262:8190-8195.

Lichtman JW, Colman H (2000) Synapse elimination and indelible memory. Neuron 25:269-278.

Luo Z, Wang Q, Dobbins GC, Levy S, Xiong WC, Mei L (2003) Signaling complexes for postsynaptic differentiation. J Neurocytol 32:697-708.

Madhavan R, Zhao XT, Ruegg MA, Peng HB (2005) Tyrosine phosphatase regulation of MuSK-dependent acetylcholine receptor clustering. Mol Cell Neurosci 28:403-416.

Maimone MM, Merlie JP (1993) Interaction of the 43 kd postsynaptic protein with all subunits of the muscle nicotinic acetylcholine receptor. Neuron 11:53-66.

Maimone MM, Enigk RE (1999) The intracellular domain of the nicotinic acetylcholine receptor alpha subunit mediates its coclustering with rapsyn. Mol Cell Neurosci 14:340-354.

Marangi PA, Wieland ST, Fuhrer C (2002) Laminin-1 redistributes postsynaptic proteins and requires rapsyn, tyrosine phosphorylation, and Src and Fyn to stably cluster acetylcholine receptors. J Cell Biol 157:883-895.

Marangi PA, Forsayeth JR, Mittaud P, Erb-Vogtli S, Blake DJ, Moransard M, Sander A, Fuhrer C (2001) Acetylcholine receptors are required for agrin-induced clustering of postsynaptic proteins. Embo J 20:7060-7073.

Martinez-Quiles N, Ho HY, Kirschner MW, Ramesh N, Geha RS (2004) Erk/Src phosphorylation of cortactin acts as a switch on-switch off mechanism that controls its ability to activate N-WASP. Mol Cell Biol 24:5269-5280.

Mittaud P, Marangi PA, Erb-Vogtli S, Fuhrer C (2001) Agrin-induced activation of acetylcholine receptor-bound Src family kinases requires Rapsyn and correlates with acetylcholine receptor clustering. J Biol Chem 276:14505-14513.

Mittaud P, Camilleri AA, Willmann R, Erb-Vogtli S, Burden SJ, Fuhrer C (2004) A single pulse of agrin triggers a pathway that acts to cluster acetylcholine receptors. Mol Cell Biol 24:7841-7854.

Mohamed AS, Swope SL (1999) Phosphorylation and cytoskeletal anchoring of the acetylcholine receptor by Src class protein-tyrosine kinases. Activation by rapsyn. J Biol Chem 274:20529-20539.

Mohamed AS, Rivas-Plata KA, Kraas JR, Saleh SM, Swope SL (2001) Src-class kinases act within the agrin/MuSK pathway to regulate acetylcholine receptor phosphorylation, cytoskeletal anchoring, and clustering. J Neurosci 21:3806-3818.

Moransard M, Borges LS, Willmann R, Marangi PA, Brenner HR, Ferns MJ, Fuhrer C (2003) Agrin regulates rapsyn interaction with surface acetylcholine receptors, and this underlies cytoskeletal anchoring and clustering. J Biol Chem 278:7350-7359.

Paoni NF, Peale F, Wang F, Errett-Baroncini C, Steinmetz H, Toy K, Bai W, Williams PM, Bunting S, Gerritsen ME, Powell-Braxton L (2002) Time course of skeletal muscle repair and gene expression following acute hind limb ischemia in mice. Physiol Genomics 11:263-272.

Podleski TR, Salpeter MM (1988) Acetylcholine receptor clustering and triton solubility: neural effect. J Neurobiol 19:167-185.

Prives J, Fulton AB, Penman S, Daniels MP, Christian CN (1982) Interaction of the cytoskeletal framework with acetylcholine receptor on th surface of embryonic muscle cells in culture. J Cell Biol 92:231-236.

Ralston E, Lu Z, Ploug T (1999) The organization of the Golgi complex and microtubules in skeletal muscle is fiber type-dependent. J Neurosci 19:10694-10705.

Roche S, Koegl M, Barone MV, Roussel MF, Courtneidge SA (1995) DNA synthesis induced by some but not all growth factors requires Src family protein tyrosine kinases. Mol Cell Biol 15:1102-1109.

Rybakova IN, Patel JR, Ervasti JM (2000) The dystrophin complex forms a mechanically strong link between the sarcolemma and costameric actin. J Cell Biol 150:1209-1214.

Sanes JR, Lichtman JW (2001) Induction, assembly, maturation and maintenance of a postsynaptic apparatus. Nat Rev Neurosci 2:791-805.

Slater CR (1982) Neural influence on the postnatal changes in acetylcholine receptor distribution at nerve-muscle junctions in the mouse. Dev Biol 94:23-30.

Smith CL, Mittaud P, Prescott ED, Fuhrer C, Burden SJ (2001) Src, Fyn, and Yes are not required for neuromuscular synapse formation but are necessary for stabilization of agrin-induced clusters of acetylcholine receptors. J Neurosci 21:3151-3160.

Stya M, Axelrod D (1983) Mobility and detergent extractability of acetylcholine receptors on cultured rat myotubes: a correlation. J Cell Biol 97:48-51.

Swope SL, Huganir RL (1993) Molecular cloning of two abundant protein tyrosine kinases in Torpedo electric organ that associate with the acetylcholine receptor. J Biol Chem 268:25152-25161.

Thomas SM, Brugge JS (1997) Cellular functions regulated by Src family kinases. Annu Rev Cell Dev Biol 13:513-609.

Thomas SM, Soriano P, Imamoto A (1995) Specific and redundant roles of Src and Fyn in organizing the cytoskeleton. Nature 376:267-271.

Twamley-Stein GM, Pepperkok R, Ansorge W, Courtneidge SA (1993) The Src family tyrosine kinases are required for platelet-derived growth factor-mediated signal transduction in NIH 3T3 cells. Proc Natl Acad Sci U S A 90:7696-7700.

Wallace BG (1992) Mechanism of agrin-induced acetylcholine receptor aggregation. J Neurobiol 23:592-604.

Wallace BG (1995) Regulation of the interaction of nicotinic acetylcholine receptors with the cytoskeleton by agrin-activated protein tyrosine kinase. J Cell Biol 128:1121-1129.

Weston C, Yee B, Hod E, Prives J (2000) Agrin-induced acetylcholine receptor clustering is mediated by the small guanosine triphosphatases Rac and Cdc42. J Cell Biol 150:205-212.

Weston C, Gordon C, Teressa G, Hod E, Ren XD, Prives J (2003) Cooperative regulation by Rac and Rho of agrin-induced acetylcholine receptor clustering in muscle cells. J Biol Chem 278:6450-6455.

Willmann R, Fuhrer C (2002) Neuromuscular synaptogenesis: clustering of acetylcholine receptors revisited. Cell Mol Life Sci 59:1296-1316.

Winder SJ, Hemmings L, Maciver SK, Bolton SJ, Tinsley JM, Davies KE, Critchley DR, Kendrick-Jones J (1995) Utrophin actin binding domain: analysis of actin binding and cellular targeting. J Cell Sci 108 (Pt 1):63-71.

Yoshihara CM, Hall ZW (1993) Increased expression of the 43-kD protein disrupts acetylcholine receptor clustering in myotubes. J Cell Biol 122:169-179.

Figure 1
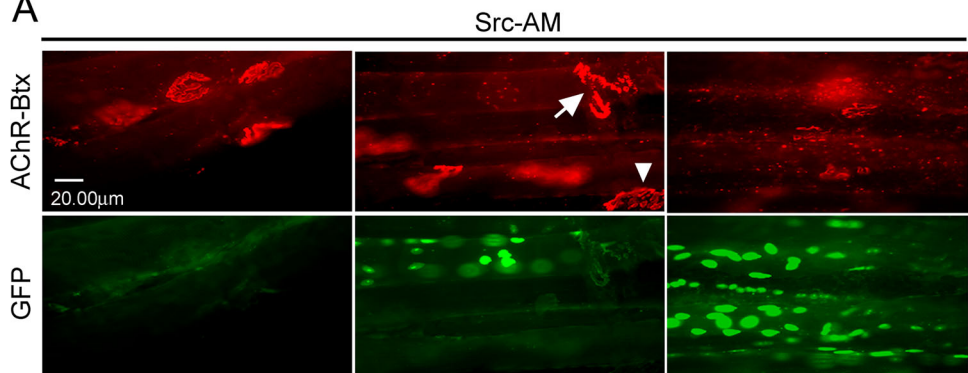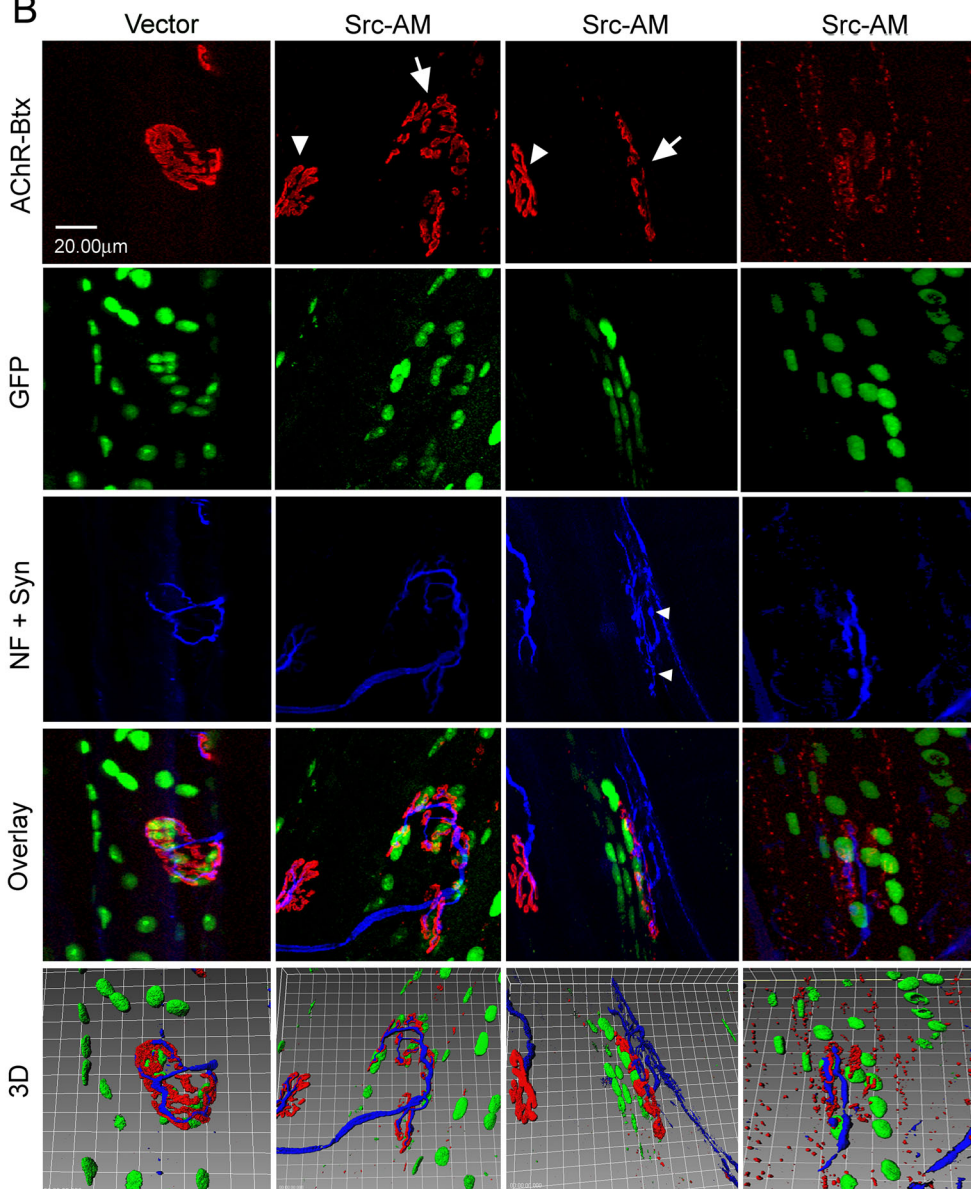
Figure 2

Vector
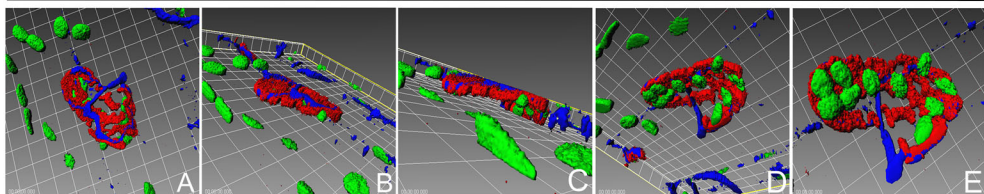
Src-AM
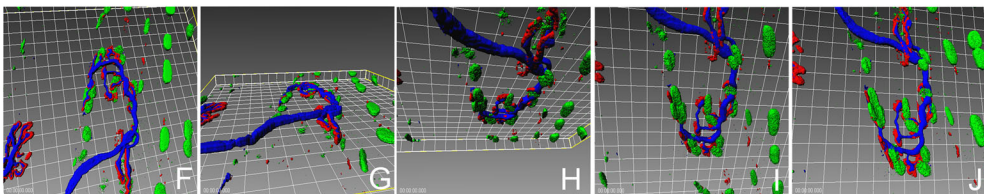
view from top

view from inside muscle

Figure 3

Figure 4

Figure 5

A

wild-type   src-/-;fyn-/-

AChR   α–DB   AChR   α–DB

AChR   Utro   AChR   Utro

AChR   Rap   AChR   Rap

AChR   α–DG   AChR   α–DG

AChR   Syntro   AChR   Syntro

AChR   PTyr   AChR   PTyr

B

- wild-type;no ag
- src-/-;fyn-/-;no ag
- wild-type;ag
- src-/-;fyn-/-;ag

Number of clusters/myotube

AChR DB Utro Syn DG Rap PTyr

C

- wild-type
- src-/-;fyn-/-

Percentage of colocalization

No ag   DB   Syn   Utro   Rap   DG   PTyr

Figure 6

Figure 7

A

	wild-type					src-/-;fyn-/-				
agrin:	−	−	+	wd 3h	wd 5h	−	−	+	wd 3h	wd 5h
		+T					+T			

Tox-P / rapsyn-blot   47−   ◄ rapsyn

AChR β− reprobe   47−   ◄ AChR β

B

C

D

Figure 8

A

	wild-type				src-/-;fyn-/-			
	control	agrin	wd 3h	wd 5h	control	agrin	wd 3h	wd 5h

Tox-P / DB-2-blot ◄ DB-2

Tox-P / α-reprobe ◄ AChRα

B

	wild-type				src-/-;fyn-/-			
	control	agrin	wd 3h	wd 5h	control	agrin	wd 3h	wd 5h

Tox-P / pTyr-blot ◄ pTyr-AChRβ

Tox-P / α-reprobe ◄ AChRα

■ wild-type
▨ src-/-;fyn-/-

***
n.s.
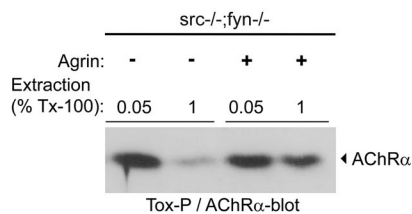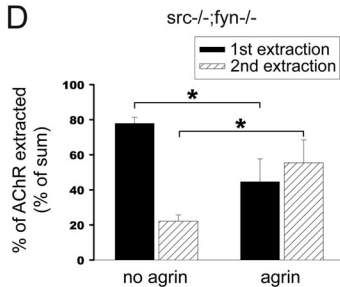*

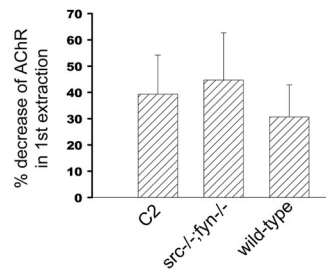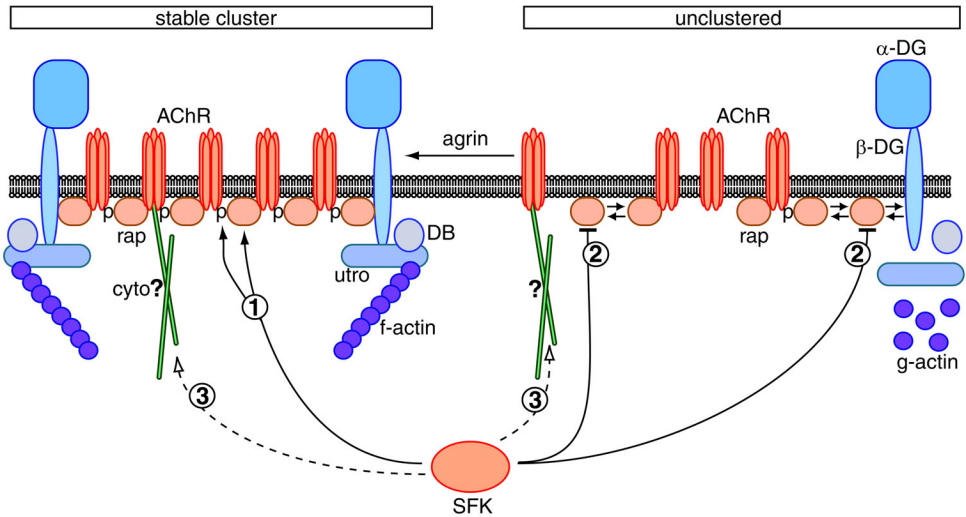phosphorylation of AChRβ (% of control)

400
300
200
100
0

control   agrin   wd 3 h   wd 5 h

Figure 9

Figure 10

Suppl. Figure 1

wild-type | src-/-;fyn-/-

AChR | α-DB | AChR | α-DB
AChR | Rap | AChR | Rap
AChR | Utro | AChR | Utro

10.00µm